

This article was downloaded by:

On: 15 January 2011

Access details: *Access Details: Free Access*

Publisher *Taylor & Francis*

Informa Ltd Registered in England and Wales Registered Number: 1072954 Registered office: Mortimer House, 37-41 Mortimer Street, London W1T 3JH, UK



## Journal of Experimental Nanoscience

Publication details, including instructions for authors and subscription information:

<http://www.informaworld.com/smpp/title~content=t716100757>

### Thermal and optical properties of poly(methyl methacrylate)/calcium carbonate nanocomposite

Z. M. Elimat<sup>a</sup>; A. M. Zihlif<sup>b</sup>; Maurizio Avella<sup>c</sup>

<sup>a</sup> Department of Applied Science, Ajloun University College, Al-Balqa Applied University, Jordan <sup>b</sup>

Department of Physics, The University of Jordan, Amman, Jordan <sup>c</sup> Institute of Chemistry and

Technology of Polymers (ICTP), CNR, Pozzuoli, Italy

**To cite this Article** Elimat, Z. M. , Zihlif, A. M. and Avella, Maurizio(2008) 'Thermal and optical properties of poly(methyl methacrylate)/calcium carbonate nanocomposite', Journal of Experimental Nanoscience, 3: 4, 259 – 269

**To link to this Article:** DOI: 10.1080/17458080802603715

**URL:** <http://dx.doi.org/10.1080/17458080802603715>

PLEASE SCROLL DOWN FOR ARTICLE

Full terms and conditions of use: <http://www.informaworld.com/terms-and-conditions-of-access.pdf>

This article may be used for research, teaching and private study purposes. Any substantial or systematic reproduction, re-distribution, re-selling, loan or sub-licensing, systematic supply or distribution in any form to anyone is expressly forbidden.

The publisher does not give any warranty express or implied or make any representation that the contents will be complete or accurate or up to date. The accuracy of any instructions, formulae and drug doses should be independently verified with primary sources. The publisher shall not be liable for any loss, actions, claims, proceedings, demand or costs or damages whatsoever or howsoever caused arising directly or indirectly in connection with or arising out of the use of this material.

## Thermal and optical properties of poly(methyl methacrylate)/calcium carbonate nanocomposite

Z.M. Elimat<sup>a\*</sup>, A.M. Zihlif<sup>b</sup> and Maurizio Avella<sup>c</sup>

<sup>a</sup>Department of Applied Science, Ajloun University College, Al-Balqa Applied University, Jordan;

<sup>b</sup>Department of Physics, The University of Jordan, Amman, Jordan; <sup>c</sup>Institute of Chemistry and Technology of Polymers (ICTP), CNR, Pozzuoli, Italy

(Received 7 August 2008; final version received 5 November 2008)

The study deals with thermal and optical properties of poly(methyl methacrylate) (PMMA) containing 2wt% calcium carbonate (CaCO<sub>3</sub>) nanofiller. It was found that the thermal conductivity increases with increasing temperatures, due to thermal activation of the phonons in the PMMA/CaCO<sub>3</sub> nanocomposite. This enhancement in the thermal conduction is mainly attributed to the heat transferred by lattice vibrations as major contributors and electrons as minor contributors during thermal conduction. The optical properties were investigated as a function of wavelength and photon energy of UV radiation. The optical results obtained were analysed in terms of absorption formula for noncrystalline materials. It was found that the measured optical energy gap for the pure PMMA is greater than the PMMA/CaCO<sub>3</sub> nanocomposite. The width of the energy tails of the localised states was calculated. Adding CaCO<sub>3</sub> nanofiller into PMMA matrix may cause the localised states of different colour centres to overlap and extend in the mobility gap. This overlap may give an evidence for decreasing energy gap when adding CaCO<sub>3</sub> nanofiller in the polymer matrix.

**Keywords:** nanocomposite; thermal conductivity; UV radiation; absorption; energy gaps

### 1. Introduction

Nanocomposites are a relatively new class of materials with ultrafine phase dimensions, typically of the order of a few nanometres. The objectives for preparation of enhanced performance nanomaterials are to obtain a homogeneous distribution of the nanoparticles within the polymer matrix, and to promote a strong interfacial adhesion between the matrix and the nanofiller. Uniform dispersion of the nanometre particles offers a major specific surface area enhancement, compared to conventional reinforcements of micrometre size. As a result, addition of small amount of a filler, compared to conventional composites, can induce dramatic changes in host matrix properties [1,2].

---

\*Corresponding author. Email: [ziad\\_elimat@yahoo.com](mailto:ziad_elimat@yahoo.com)

Recently, nanoparticles attracted great interest because, when they are added to polymers, they create environmentally friendly polymers that can be utilised in the fabrications of advanced materials, especially in the biotechnology world where medical devices and packaging boxes are of great interest [3–5]. Nanocomposites could dramatically induce improvements in mechanical and electrical properties, heat resistance, radiation resistance and other areas as a result of the nanometre-sized dispersion of the inorganic fillers in the organic matrix [6–10]. An immense amount of research and development has been devoted to characterising and understanding the mechanical and physical properties of such nanocomposites. In recent years, studies on the optical, thermal and electrical properties of polymer nanocomposites have attracted much attention in view of their important applications in optical devices. The optical properties of polymers can be enormously modified by addition of nanoparticles, which react effectively with the host matrix due to their very large surface areas with respect to macro/microparticles. Thus, addition of such nanoparticles such as titanium dioxide ( $\text{TiO}_2$ ), potassium chlorate ( $\text{KClO}_3$ ), calcium carbonate ( $\text{CaCO}_3$ ), and potassium iodate ( $\text{KIO}_3$ ) to a polymeric system may be expected to enhance its optical and electrical performance [6].

Calcium carbonate and other layered silicates in nanosize dimension have been commonly used in preparation of highly performance nanocomposites with large specific surface areas. The nanometre-sized commercially available  $\text{CaCO}_3$  has been used merely to reduce the cost of expensive resins; however, the improvement in various properties such as the mechanical property of micrometre-size  $\text{CaCO}_3$ -filled composites is believed to be poor due to the decrease of the polymer–filler interaction [6,11].

In the study of physical properties of polymers, the optical absorption spectrum is one of the most important tools for understanding band structure and electronic properties of pure and filled polymers. This technique depends on the transition of some electrons from the valence band (VB) to the conduction band (CB), when photon energy is greater than the band energy. The transition is direct when the wave vector for the electron remains unchanged, but in the case of indirect transition, interaction with a lattice vibration (phonon) occurs (the minimum of the CB lies in a different part of  $K$ -space from the maximum of the VB) [12,13]. As a consequence, the nanocomposite properties are strongly influenced by the nature of the interface between inorganic and polymer matrices. A strong interfacial interaction between the inorganic nanoparticles and the polymer matrix can give rise to some unusual properties in these materials [14,15].

Avella et al. [16] succeeded in the preparation of novel poly(methyl methacrylate) (PMMA)/ $\text{CaCO}_3$  nanocomposites by an *in situ* polymerisation process with a very fine dispersion and a good interfacial adhesion between the two phases. The exhibited performance of the examined properties of the nanocomposites as glass temperature, abrasion resistance, and morphology was quite different from the conventional microcomposites. Furthermore, they claimed from the observed scanning electron microscope (SEM) morphology that the nanoparticles are completely covered by the PMMA matrix and the material appears as a one-phase system. To the best of our knowledge, little attention has been paid to the study of the thermal conductivity and optical properties of the  $\text{CaCO}_3$  nanocomposites. The present work is part of a systematic study of the effect of the addition of a nanofiller into a polymer matrix for the purpose of characterising the thermal and optical properties of PMMA/ $\text{CaCO}_3$  nanocomposites.

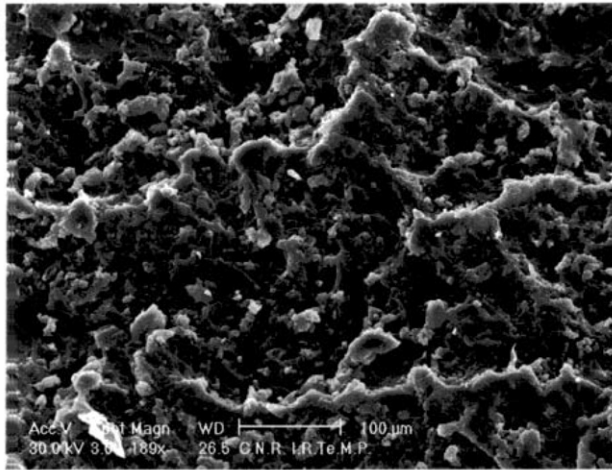
## 2. Experimental work

### 2.1. Material preparation

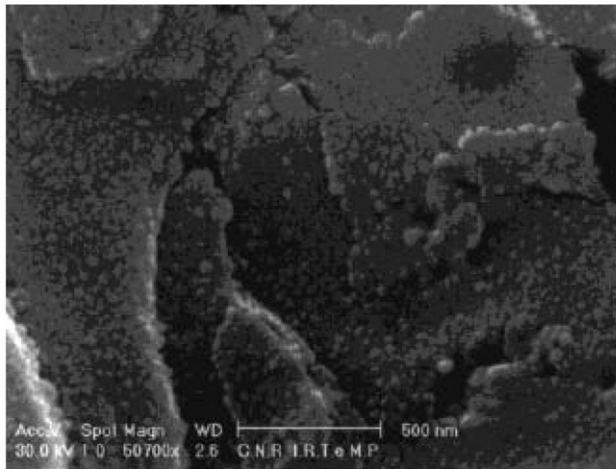
The PMMA/CaCO<sub>3</sub> nanocomposites were prepared by an *in situ* polymerisation. Precipitated CaCO<sub>3</sub> nanoparticles covered by stearic acid, commercialised under the trademark SOCAL (Solvay & Cie), with a mean size of about 40 nm as fillers, were used. The presence of stearic acid as organic coating on the nanofiller surface confers hydrophobic properties to CaCO<sub>3</sub> that can improve its compatibility with the polymeric matrix. In particular, the experimental conditions of the sample preparation were as follows. Step 1 – In a cylindrical reactor equipped with inlets for refrigeration, mechanical stirring, and nitrogen, kept in an oil bath at 90°C, methyl methacrylate containing 1wt% of dicumylperoxide, previously dissolved, was added. To this solution, 2wt% of CaCO<sub>3</sub> nanoparticles was added. This solution was stirred mechanically at 90°C until a critical viscosity that corresponds to a prepolymerisation of the monomer was reached. It was observed that the time it takes to achieve a critical viscosity value was related to the amount of nanoparticles. Step 2 – The viscous mixture was then inserted into a mold and kept at 100°C for 24 h to complete the polymerisation process. Finally, the nanocomposite so obtained was kept for 4 h at 140°C to be sure that the entire prepolymer fraction had been converted. Monomer polymerisation has been promoted by thermal decomposition of the organic peroxide during the blending. Generally, acrylic polymerisation is carried out in suspension, and the suspending medium is a salt-water solution. Due to the incompatibility of the nanoparticles with water, in this case methyl methacrylate polymerisation has been performed in bulk [13]. To establish the degree of nanoparticle dispersion within the polymeric matrix, nanocomposite samples were cryogenically broken after immersion in liquid nitrogen and the fractured surfaces were observed by SEM [16]. This analysis was carried out with a Philips SEM 501 electron microscope, and the scanning electron micrographs were taken on Au/Pd-coated fractured surfaces of the dumbbell specimens. The effects of CaCO<sub>3</sub> nanoparticles on mechanical properties of PMMA/CaCO<sub>3</sub> nanocomposites have been analysed and the data are summarised in Table 1 [16]. In Figure 1(a) and (b), the SEM micrographs of the fractured surfaces of the neat PMMA and nanocomposites containing 2wt% of the CaCO<sub>3</sub> nanoparticles are shown as examples. From the figures it can be observed that the nanoparticle size ranges between 40 and 70 nm. The tiny small black dots refer to the nanofiller CaCO<sub>3</sub> [16].

Table 1. Flexural properties and glass transition temperature of neat PMMA and PMMA/CaCO<sub>3</sub> nanocomposite.

Material	Flexural modulus (MPa)	Ultimate strength (MPa)	Ultimate strain	Glass transition temperature $T_g$ (°C)
PMMA	1880	19	0.0137	90
PMMA/CaCO <sub>3</sub>	2450	18	0.0102	120



(a)



(b)

Figure 1. (a) SEM micrograph for neat PMMA polymer fractured surface. (b) SEM micrograph for PMMA/CaCO<sub>3</sub> nanocomposite fractured surface.

## 2.2. Thermal properties measurements

The measurements of the thermal conductivity were carried out using a computerised thermal conductivity apparatus (Figure 2). This apparatus measures the thermal conductivity using Heat Flowmeter Steady-State Method. The specimen was sandwiched between two rubber sheets to remove the air gaps, and then it was placed between a hot plate and the heat flowmeter, which is attached to a cold plate. The hot and cold plates are maintained at constant temperatures, the temperature of the two plates was measured using surface thermocouples. The apparatus is surrounded by an insulating jacket to minimise the heat loss.

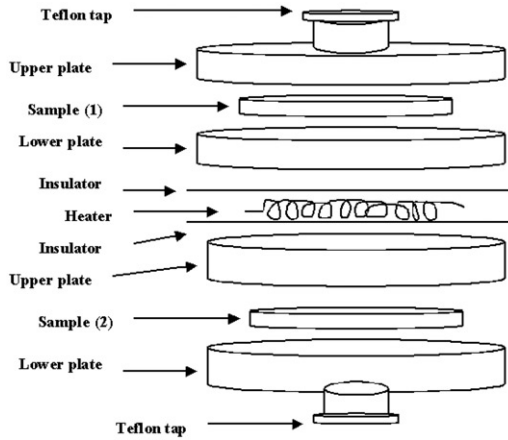


Figure 2. Thermal conductivity apparatus.

Thermal conductivity represents the amount of heat energy conducted per unit time through a unit area (perpendicular to the direction of heat transfer) when the temperature gradient across the heat-conducting element is one unit. Conduction of heat in insulating solids can be due to thermally excited lattice vibrations (phonons), thus the thermal conductivity is caused by phonon conductivity as a major contributor as a result of the molecular vibration of the lattice where there are little free electrons in the nanocomposite [16,17]. The thermal conductivity ( $k$ ) can be found from the familiar relation [18]:

$$\frac{dq}{dt} = -Ak \frac{dT}{dL} \tag{1}$$

where  $dq/dt$  is the rate of heat flow transported as a result of the temperature gradient  $-dT/dL$  since  $T_1 > T_2$ , and  $A$  is the sample cross-section area.

Under steady-state condition, the temperature gradient becomes  $(\Delta T/\Delta L)$ , and the heat flow  $(\Delta q/\Delta t)$  becomes [18]:

$$\frac{\Delta q}{\Delta t} = -kA \left( \frac{\Delta T}{\Delta L} \right) \tag{2}$$

where  $\Delta T = T_2 - T_1$  is the temperature difference between the specimen faces, and  $\Delta L$  is the specimen thickness.

The quasi-state temperature difference  $\Delta T_s$  were found to be identical for the thermocouple pairs on one side, and those on the other sides. This gives support to the assumption of symmetry on both sides of the heat flux. The values of thermal conductivity ( $k$ ), at each temperature, were calculated from the relation:

$$k = q_s \left( \frac{L}{\Delta T_s} \right) = \frac{IVL}{2A\Delta T_s} \tag{3}$$

where  $q_s$  are the heat flux,  $I$  the electrical current,  $V$  the electrical voltage, and  $A$  the area of the heating foil. The factor 2 is due to the symmetrical distribution of heat flux on both

sides of the apparatus [19]. This is because we used two circular disks of identical thickness. The thermal resistivity ( $r$ ) is the reciprocal of the thermal conductivity [18]:

$$r = \frac{1}{k} (\text{m}^2 \text{C W}^{-1}). \quad (4)$$

The thermal resistance ( $R$ ) is given by the equation:

$$R = \frac{L}{k} (\text{m}^2 \text{C W}^{-1}). \quad (5)$$

### 2.3. Optical absorption measurements

The most direct and the simplest method for probing the band structure of materials is to measure the absorption spectrum. In the absorption process, a photon of known energy excites an electron from a lower to a higher energy state. Studying the changes in transmitted radiation, one can decide the types of possible transitions an electron can make. Fundamental absorption refers to band-to-band or to exciting transitions. The fundamental absorption manifests itself by a rapid rising in absorption, known as the absorption edge, and can be used to determine the optical energy gap. Absorption is expressed in terms of a coefficient  $\alpha(\nu)$ , which is defined as the relative rate of decrease in the light intensity.

The optical absorbance  $A(\nu)$  spectra of nanocomposite were collected at room temperature in the wavelength range 200–800 nm with UV-visible spectrophotometer. The absorption coefficient  $\alpha(\nu)$  was calculated from the absorbance  $A(\nu)$ . After correction for reflection  $\alpha(\nu)$  was calculated using the relation:

$$I = I_0 \exp(-\alpha x). \quad (6)$$

Hence

$$\alpha(\nu) = \frac{2.303}{x} \log\left(\frac{I_0}{I}\right) = \frac{2.303}{x} A(\nu) \quad (7)$$

where  $I_0$  and  $I$  are the incident and transmitted intensity, and  $x$  is the sample thickness [20–22].

The relationship between fundamental absorption and optical energy gap is given by the relation:

$$E_{\text{opt}} = \frac{hc}{\lambda} \quad (8)$$

where  $c$  is the velocity of light.

At high absorption coefficient levels for noncrystalline materials can be related to the energy of the incident photon as follows:

$$\alpha(\nu) = \beta(h\nu - E_{\text{opt}})^r \quad (9)$$

where  $\beta$  is constant and the exponent  $r$  can assume values of 0.5, 1, 2, 3, and 3/2. For allowed indirect transition the exponent takes the values 1, 2, and 3. At low absorption

levels, in the range of  $1\text{--}10^{-4}\text{ cm}^{-1}$ , the absorption coefficient  $\alpha(\nu)$  is described by the Urbach formula [13]

$$\alpha(\nu) = \alpha_0 \exp\left(\frac{h\nu}{\Delta E}\right) \quad (10)$$

where  $\alpha_0$  is a constant and  $\Delta E$  is an energy which is interpreted as the width of the tail of localised state of the forbidden band gap [20–22].

### 3. Results and discussions

Figure 3 shows the variation of thermal conductivity *versus* temperature for PMMA/ $\text{CaCO}_3$  composite. It is clearly shown that the thermal conductivity increases with increasing temperatures, due to thermal activation of the phonons in the PMMA/ $\text{CaCO}_3$  composite. We observed that the thermal conductivity was affected most by the addition of 2wt%  $\text{CaCO}_3$  to neat PMMA polymer. It was found that the thermal conductivity of neat PMMA increased from  $0.168\text{ W m}^{-1}\text{K}^{-1}$  to  $0.175\text{ W m}^{-1}\text{K}^{-1}$  with the addition of 2wt%  $\text{CaCO}_3$ , which indicates that the composite conduct heat is better than neat PMMA. We must point out the enhancement in the thermal conduction is mainly attributed to the heat transferred by lattice vibrations as (major contributors) and electronic contribution as (minor contributors) during thermal activation. The increase of thermal conductivity to PMMA with temperature is typical to that of the amorphous polymers. The variation of thermal resistance *versus* temperature shown in Figure 4, in which it decreases with increasing temperature.

Optical absorption studies on neat PMMA and PMMA/ $\text{CaCO}_3$  nanocomposite as shown in Figure 5 were carried out to obtain energy-band gaps of the samples, the optical spectra were recorded at room temperature.

The plots of  $(\alpha h\nu)^2$  *versus* photon energy  $h\nu$  were used to evaluate the optical gaps. A typical plot is shown in Figure 6 [23,24]. The best fitting to the absorption spectra in Equation (9) gave  $r = (1/2)$ , meaning the electron transition allowed direct transition for these nanocomposite samples.

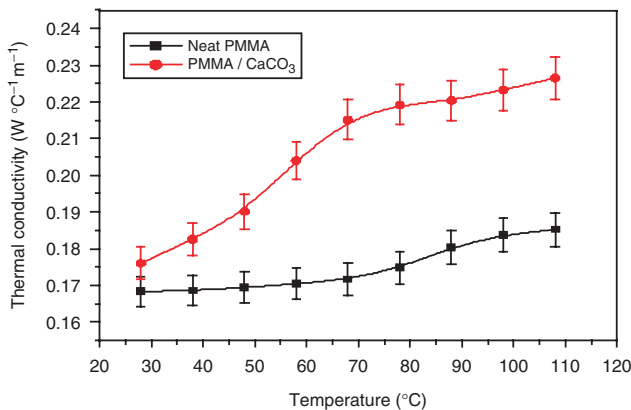


Figure 3. Shows the variation of thermal conductivity vs. temperature for PMMA/ $\text{CaCO}_3$  nanocomposite.



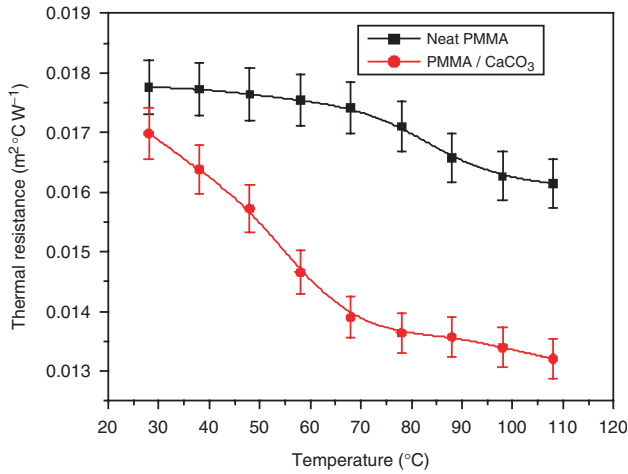


Figure 4. The variation of thermal resistance vs. temperature for PMMA/CaCO<sub>3</sub> composite.

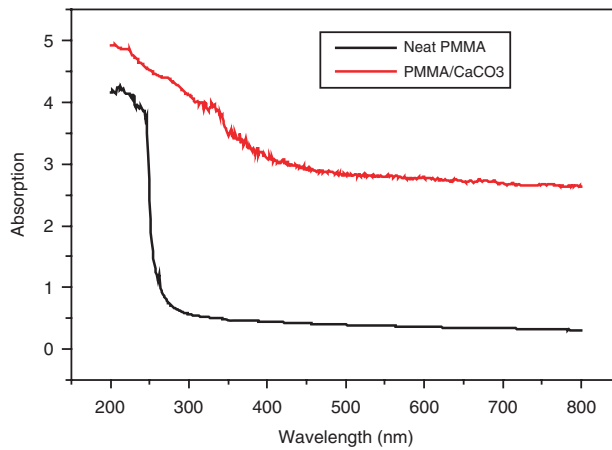


Figure 5. The optical absorption spectra for PMMA/CaCO<sub>3</sub> composite.

It can be seen that the plot is linear in the region of strong absorption near the fundamental absorption edge. Thus, the absorption takes place through direct transition. The band gap obtained by extrapolating the linear part to zero of the ordinate is also indicated in the figure. The band gaps,  $E_g$ , were evaluated in this way and the slope gives the value of constant  $\beta$ . The factor  $\beta$  depends on the transition probability and can be assumed to be constant within the optical frequency range.

Adding CaCO<sub>3</sub> in PMMA matrix may cause the localised states of different colour centres to overlap and extend in the mobility gap. This overlap may give us an evidence for decreasing energy gap when adding CaCO<sub>3</sub> in the polymer matrix [25].

The Urbach formula Equation (10) was used to calculate the width of the urbach tail of the localised states due to the defect levels in the transition gap [20]. The linear dependence

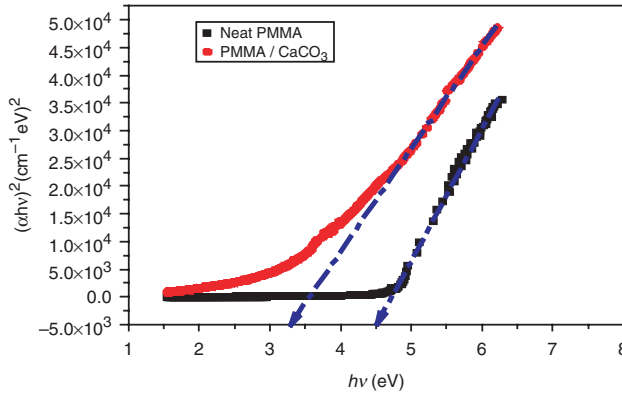


Figure 6. Evaluated  $E_g$  from optical absorption spectra of the samples.

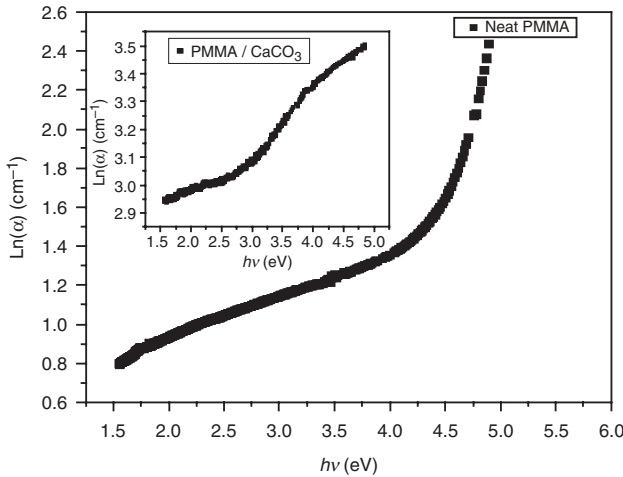


Figure 7. The linear dependence of  $\ln \alpha$  vs.  $h\nu$ .

Table 2. The obtained optical data of neat PMMA and PMMA/CaCO<sub>3</sub>.

Material	$E_{opt}$ (eV)	$\beta$	$\Delta E$ (eV)
PMMA	4.50	150	0.221
PMMA/CaCO <sub>3</sub>	3.32	135	0.318

of  $\ln \alpha$  versus  $h\nu$  is presented in Figure 7. The reciprocal of the slopes of the curves yields the magnitude of width of the band tail,  $\Delta E$ , and the value of  $\Delta E$  for pure PMMA is 0.221 eV and 0.318 for PMMA/CaCO<sub>3</sub> composite. It is observed that the Urbach tail for pure PMMA is less than that for PMMA/CaCO<sub>3</sub> composite. Table 2 summarises the obtained optical data.

#### 4. Conclusions

In the present study, thermal and optical properties of PMMA/CaCO<sub>3</sub> nanocomposite were investigated and the following conclusions can be obtained:

- (1) The thermal conductivity increases with increasing temperatures.
- (2) The thermal conductivity of neat PMMA increased with the addition of 2wt% CaCO<sub>3</sub> nanofiller, which indicate that the composite conduct heat is better than neat PMMA.
- (3) The enhancement in the thermal conduction is mainly attributed to the heat transferred by lattice vibrations as (major contributors) and electronic contribution as (minor contributors) during thermal activation.
- (4) The best fitting to the absorption spectra gave  $r = (1/2)$ , meaning it allowed direct transition for these samples.
- (5) Adding CaCO<sub>3</sub> nanofiller in PMMA matrix may cause the localised states of different colour centres to overlap and extend in the mobility gap. This overlap may give us an evidence for decreasing energy gap when adding CaCO<sub>3</sub> in the polymer matrix.
- (6) It is observed that the Urbach tail for pure PMMA is less than that for PMMA/CaCO<sub>3</sub> composite.

#### References

- [1] E.P. Giannelis, *Polymer layered silicate nanocomposites*, Adv. Mater. 8 (1996), pp. 29–35.
- [2] M. Avella, S. Cosco, M.L. Di Lorenzo, E. Di Pace, and M.E. Errico, *Influence of CaCO<sub>3</sub> nanoparticles shape on thermal and crystallization behavior of isotactic polypropylene based nanocomposites*, J. Thermal Anal. Calorimetry 80 (2005), pp. 131–136.
- [3] J. Gersten and F. Smith, *The Physics and Chemistry of Solids, Nanostructures*, John Wiley and sons, INC, New York, 2001, p. 383.
- [4] M. Batraton, *Synthesis, Fictionalization and Surface Treatment of Nanoparticles*, Chap. 8, American Scientific Publishers, California, 2003.
- [5] Y. Zhou and Y. Lin, *Optical and dielectric properties of a nanostructured NbO<sub>2</sub> thin film prepared by thermal oxidation*, Phys. D Appl. Phys. 37 (2004), pp. 3392–3395.
- [6] H. Sawada, Y. Shikauchi, H. Kakehi, Y. Katoh, and M. Miura, *Preparation and applications of novel fluoroalkyl end-capped oligomers/calcium carbonate nanocomposites*, Colloid. Polym. Sci. 285 (2007), pp. 499–506.
- [7] M. Zanetti, S. Lomakin, and G. Camino, *Polymer layered silicate nanocomposites*, Macromol. Mater. Eng. 279 (2000), pp. 1–9.
- [8] G. Schmid (ed.) *Nanoparticles – from Theory to Application*, Wiley-VCH, Weinheim, 2004.
- [9] P.M. Ajayan, L.S. Schadler, and P.V. Braun, *Nanocomposite Science and Technology*, Wiley-VCH, Weinheim, 2003.
- [10] P. Gomez-Romero and C. Sanchez, *Functional Hybrid Materials*, Wiley-VCH, Weinheim, 2004.
- [11] C.M. Chan, J. Wu, J.X. Li, and Y.K. Cheung, *Polypropylene/calcium carbonate nanocomposites*, Polymer 43 (2002), pp. 2981–2992.
- [12] R. Murri, L. Schiavulli, N. Pinto, and T. Ligonzo, *Urbach tail in amorphous gallium arsenide films*, J. Non-Cryst. Solids 139 (1992), pp. 60–66.

- [13] F. Urbach, *The long-wavelength case of photographic sensitivity and of the electronic absorption of solids*, Phys. Rev. 92 (1953), p. 1324.
- [14] X. Qiang, Z. Chunfang, Y. JianZun, and C.S. Yuan, *The effects of polymer-nanofiller interactions on the dynamical mechanical properties of PMMA/CaCO<sub>3</sub> composites prepared by microemulsion template*, J. Appl. Polym. Sci. 91 (2004), pp. 2739–2749.
- [15] S. Bose, R. Pandey, M.B. Kulkarni, and P.A. Mahanwar, *Effect of talc and synthetic sodium aluminum silicate (SSAS) on the properties of poly (methyl methacrylate)*, J. Thermoplast. Compos. Mater. 18 (2005), pp. 393–405.
- [16] M. Avella, M.E. Errico, and E. Martuscelli, *Novel PMMA/CaCO<sub>3</sub> nanocomposites abrasion resistant prepared by an in situ polymerization process*, Nano Lett. 1 (2001), pp. 213–217.
- [17] E.P. Sakandiou, H.R. Van Den Berg, and C.A. Ten Seldam, *Thermal conductivity of Methan in the critical region*, J. Chem. Phys. 1058(23) (1996), pp. 10535–10555.
- [18] D. Tabor, *Gasses, Liquids and Solids*, Arrowsmith, London, 1995.
- [19] T. Katsure and M.R. Kamal, *Electrical and thermal properties of polypropylene filled with steel fiber*, Adv. Polymer Tech. 5 (1987), pp. 193–202.
- [20] E.A. Daris and N. Mott, *Conduction in noncrystalline systems. V. Conductivity, optical absorption, and photoconductivity in amorphous semiconductors*, Phil. Mag. 22 (1970), pp. 903–922.
- [21] S.K.J. Al-Ani and A.M. Zihlif, *Optical properties of epoxy-glass microballoons composite*, Optic. Mater. 59 (1996), pp. 69–73.
- [22] N.F. Mott and E.A. Davis, *Electronic Processes in Non-crystalline Materials*, Clarendon Press, Oxford, England, 1971.
- [23] X. Ma, B. Zhou, Y. Deng, Y. Sheng, C. Wang, Y. Pan, and Z. Wang, *Study on CaCO<sub>3</sub>/PMMA nanocomposite microspheres by soapless emulsion polymerization*, Colloid. Surface A: Physicochem. Eng. Aspect. 312 (2008), pp. 190–194.
- [24] S.K. Medeiros, E.L. Albuquerque, F.F. Maia Jr, E.W.S. Caetano, and V.N. Freire, *Electronic and optical properties of CaCO<sub>3</sub> calcite, and excitons in Si@CaCO<sub>3</sub> and CaCO<sub>3</sub>@SiO<sub>2</sub> core-shell quantum dots*, J. Phys. D: Appl. Phys. 40 (2007), pp. 5747–5752.
- [25] H.M. Zidan and M. Abu-Elnader, *Structural and optical properties of pure PMMA and metal chloride-doped PMMA films*, Physica B 355 (2005), pp. 308–317.